JOURNAL OF GEOPHYSICAL RESEARCH, VOL. 87, NO. B12, PAGES 9747–9754, NOVEMBER 30, 1982

New Radar-Derived Topography for the Northern Hemisphere of Mars

G. S. DOWNS,[1] P. J. MOUGINIS-MARK,[2] S. H. ZISK,[3] AND T. W. THOMPSON[4,5]

Earth-based radar altimetry data for the northern equatorial belt of Mars (6°S–23°N) have recently been reduced to a common basis corresponding to the 6.1-mbar reference surface. A first look at these data indicates that the elevations of Tharsis, Elysium, and Lunae Planum are lower (by 2–5 km) than has been suggested by previous estimates. These differences show that the required amount of tectonic uplift (or constructional volcanism) for each area is less than has been previously envisioned. Atmospheric or surficial conditions are suggested which may explain the discrepancies between the radar topography and elevations measured by other techniques. The topographies of Chryse Planitia, Syrtis Major, and Valles Marineris are also described.

INTRODUCTION

For each Mars opposition between 1971 and 1980, earth-based radar measurements made at 3.5-cm (*X* band) and/or 12.6-cm (*S* band) wavelengths have provided detailed information on the topography and surface characteristics of the planet. During this period, segments of the Martian surface within ±23° of the equator were investigated (Figure 1), permitting hemispheric variations in the radar properties to be studied. Detailed descriptions of the data collection and processing techniques for the 1971, 1973, and 1975/1976 Goldstone measurements of Mars have been given by *Downs et al.* [1975] and *Roth et al.* [1980], to which the reader is referred. Data for the 1978 and 1980 oppositions were processed by techniques similar to those employed for the earlier oppositions.

Two of us (G.S.D., T.W.T.) have recently reduced the measurements of surface topography made during these five Mars oppositions to the elevation datum corresponding to the 6.1-mbar atmospheric pressure surface [*Wu*, 1978]. The elevation of each point was obtained by combining the distance to the surface (calculated from the time delay of the peak power in the measured delay function) with the radius of the 6.1-mbar datum at the given latitude and longitude. The Jet Propulsion Laboratory ephemeris DE-114 was used for computing the time delay to the Martian center of mass and the areographic coordinates of the subearth point. Using range–Doppler frequency analysis, the radar signal for each opposition was partitioned into echoes from small, well-defined areas of the surface. The size of each resolution cell was dependent upon the parameters of the radar experiment (such as distance to the planet and transmitter power), permitting areas measuring 10–30 km (0.16°–0.5°) in longitude and 80–120 km (1.3°–2.0°) in latitude to be analyzed.

The purpose of this paper is, first, to present in a timely manner these new radar elevation measurements for regions where differences appear between these and earlier results; second, to discuss in general terms the significance of the data in the study of the Martian crust and of its history; and, finally, to suggest atmospheric or surficial conditions which may explain the discrepancies between the radar topography and that measured by other techniques.

[1]Jet Propulsion Laboratory, Pasadena, California 91109.
[2]Department of Geological Sciences, Brown University, Providence, Rhode Island 02912.
[3]NEROC Haystack Observatory, Westford, Massachusetts 01886.
[4]Planetary Science Institute, Science Applications, Incorporated, Pasadena, California 91101.
[5]Now at Jet Propulsion Laboratory, Pasadena, California 91109.

Paper number 2B0641.
0148-0227/82/002B-0641$05.00

TOPOGRAPHIC PROFILES

The largest discrepancy between the radar topography and the previously published topographic data, derived primarily from the Mariner 9 radio occultation data [*Kliore et al.*, 1972, 1973; *Wu*, 1978], appears to be in the northern hemisphere where no radar data were available at the time when the topographic map was published. Because many geological and geophysical investigations have focused on the northern hemisphere, we have selected three such areas where the elevation discrepancy exists to illustrate the new radar data set and present here some preliminary observations.

Tharsis. The Tharsis region has been the center of numerous analyses [*Carr*, 1974; *Wise et al.*, 1979*a*; *Phillips and Lambeck*, 1980; and others], due to the presence of the four large, morphologically fresh shield volcanoes and the apparent elevated nature of the area. Nearly continuous radar profiles that cross Tharsis close to the summit of Ascraeus Mons (9.6°–12.1°N), together with additional data for the same longitude range at 21.6°N, were acquired at Goldstone and are shown in Figures 2*a*–2*c*. Profiles from the U.S. Geological Survey topographic map of Mars (miscellaneous map I-961) are included for comparison. There is a disparity between the two data sets which appears to be greatest at about 12°N, 111°W, where the lava plains immediately to the west of Ascreaus Mons are at an elevation of 3.65 km (nearly 6 km lower than has previously been believed). At 9.6°N, 111°W, the base of Ascraeus Mons is shown by the radar data to be at an elevation of 4.43 km, indicating that there is a northward dipping slope west of the volcano. In general, the mean elevation of the northern portion of the Tharsis dome (about 4000 km in diameter) appears to be about 2–3 km lower than previous measurements suggested, although the lava plains surrounding Arsia Mons (which comprise the southern portion of the dome) are at elevations of 9–11 km [*Mouginis-Mark et al.*, 1982]. It now seems possible that the northern part of Tharsis could have been formed by the eruption of successive lava flows which produced a lava sequence perhaps 2–3 km thick [*Solomon and Head*, 1980], although some form of tectonic uplift to support the large, uncompensated crustal load [*Phillips et al.*, 1973; *Phillips and Saunders*, 1975; *Lambeck*, 1979; *Sleep and Phillips*, 1979] is also possible. This relatively thin sequence of lavas is also consistent with the estimates of flow thicknesses by *Pike and Clow* [1981], based on morphometric analyses of

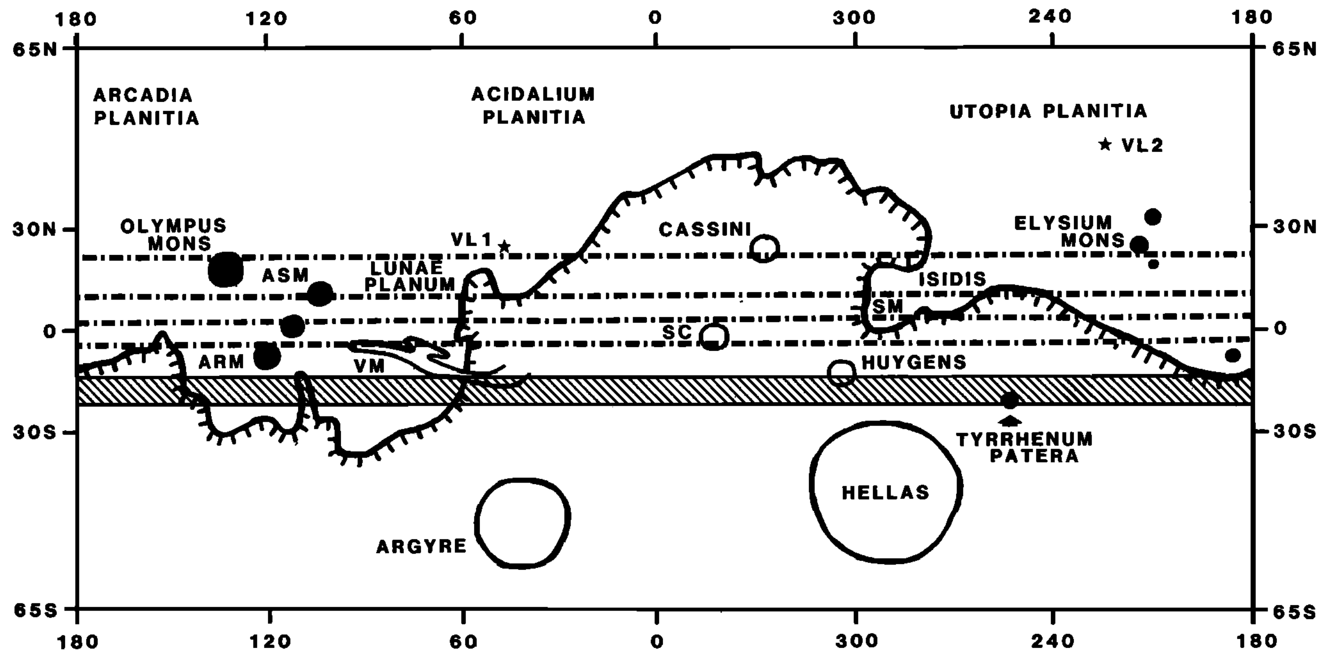

Fig. 1. Sketch map (Mercator projection) of the areas of Mars covered by the Goldstone radar data set presented here. Dot-dashed lines represent latitudes for which partial radar coverage was obtained (some data are missing for areas within Tharsis and Elysium) for latitude bands approximately 3° in width. Cross-hatched band between 14° and 22°S has almost complete radar coverage for the entire circumference of the planet. Solid circles show the locations of the younger volcanic constructs, open circles are large impact basins, and the barbed line represents the highland-lowland boundary scarp. Abbreviations are as follows: ARM, Arsia Mons; ASM, Ascraeus Mons; SC, Schiaparelli; SM, Syrtis Major Planitia; VL1 and VL2, Viking Lander 1 and 2 sites; and VM, Valles Marineris.

the small volcanic shields in this area (e.g., Biblis and Ulysses Paterae). The measurements by Pike and Clow indicate that the shields never possessed basal diameters much greater than their present dimensions and, as inferred from the geometry of their flanks, were only flooded by a thin layer of younger flows. As in the case of Tharsis, the Elysium dome is shown by the radar measurements (Figure 2*d*) to be lower (by 1–2 km) than has previously been estimated. No elevation measurements were acquired for the summit of Elysium Mons, but a groundtrack at 22.3°N (about 150 km south of the summit) gave a mean elevation of 4.58 km for the southern flanks of the volcano between 212° and 214°W. A very steep local slope (about 1.67°) is located on the western edge of the Elysium dome; the elevation changes from +3.13 km at 22.1°N, 219.0°W, to −1.01 km at 22.1°N, 225.0°W. Were this steep slope to continue to the north, it is possible that it represents a contributing factor in the formation of the Elysium Fossae channels, which are a unique set of Martian channels situated about 120 km to the north [*Mouginis-Mark and Brown*, 1981].

Lunae Planum and Chryse Planitia. The radar groundtracks over Lunae Planum (Figure 3) also indicate a lower elevation than did earlier interpretations. Rather than being a plateau at an elevation of 4–5 km, Lunae Planum now seems to have an altitude of 1–2 km above the 6.1-mbar reference surface, with a gentle slope down toward the east. It may also be significant that Lunae Planum is elevated only 1–1.5 km above the heavily cratered terrain found at longitudes 40°–55° and 15°–25°W (Figure 3*b*). Recent measurements of the Lunae Planum lavas [*De Hon*, 1981] have indicated that these flows also probably have a thickness of 1–1.5 km, suggesting that the ridged plains materials in this area may have been simply emplaced on top of preexisting cratered terrains. Crustal foundering (as a consequence of mantle overturning or first-order convection) with erosional retreat of the highland boundary scarp [*Wise et al.*, 1979*b*] has been suggested as a possible mechanism for generating the hemispheric asymmetry on Mars. The possible existence of buried cratered terrain beneath the Lunae Planum lavas would, however, argue against such a large-scale reworking of the Martian crust because the original highland material is apparently preserved.

In the region south of Chryse Planitia (Figure 3*b*) the surface elevation as measured by the radar is approximately −2 km, or about 1 km lower than has been reported earlier. In addition, the two profiles presented in Figure 3 show that the channels within Simud and Tiu valles (located about 600 km to the south of Chryse Planitia) have carved valleys to about the same level as Chryse (that is, the channel floors are about 2 km below Mars datum). If the present relief of this area is assumed to be representative of the earlier topography over which the big channel systems were formed (and were transporting material), then the very small regional slopes may have restricted the areal distribution of the larger channel-carried boulders, particularly in the distal areas of the outwash plains. This observation may be significant when the inferred mode of emplacement and origin of the boulders at the Viking Lander 1 site are considered. The boulders at this locality have a much larger range of sizes and shapes than the rocks observed at the Viking Lander 2 site [*Garvin et al.*, 1981], and such a difference had been tentatively attributed in part to a fluvial transport mechanism depositing a greater diversity of boulders at the Viking Lander 1 site [*Garvin et al.*, 1981]. If the regional slopes south of Viking Lander 1 were very shallow, however, this transport mechanism for the boulders may have been less efficient than has previously been believed, necessitating an alternative explanation for the origin of the boulder field. In

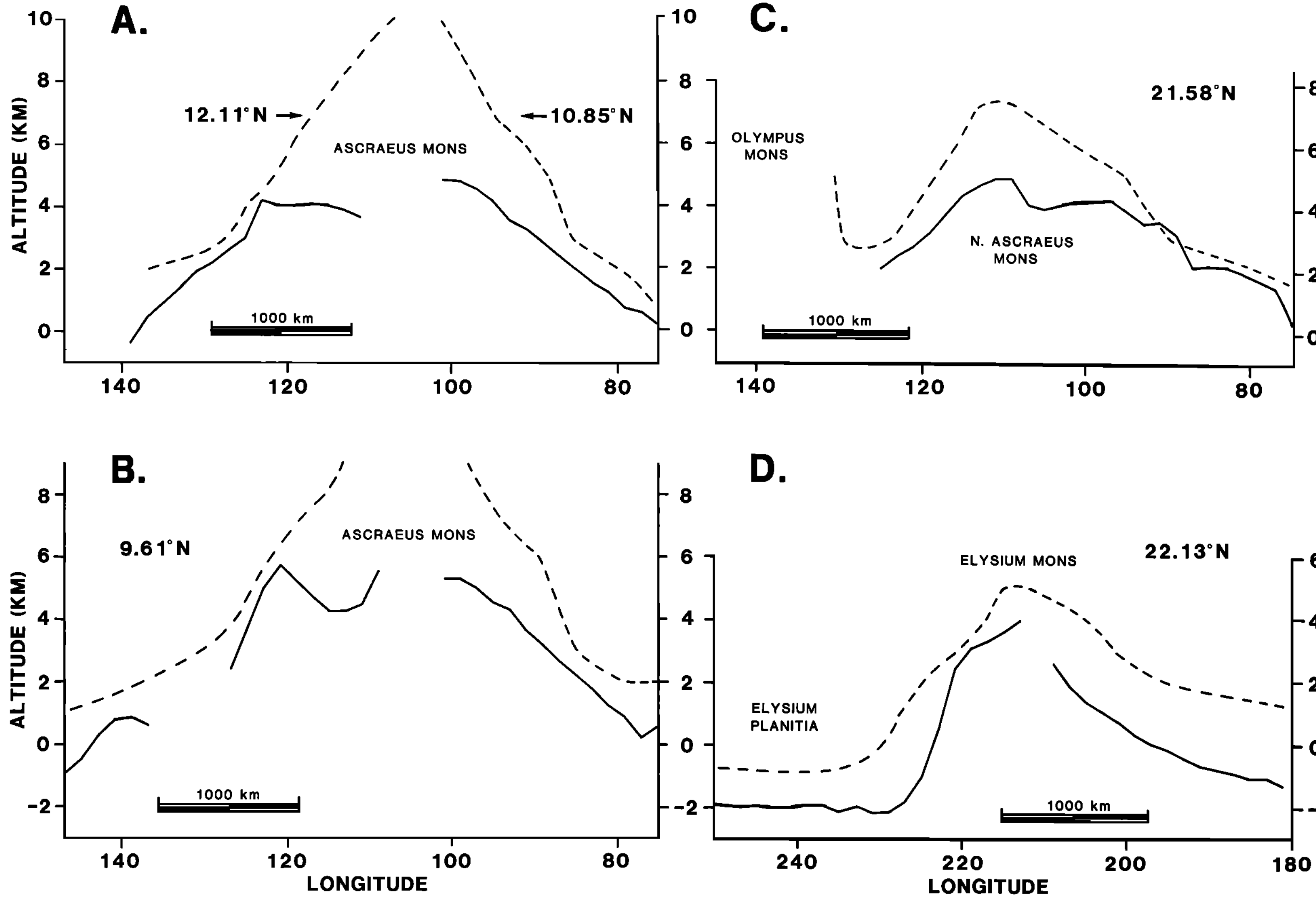

Fig. 2. (*a–c*) Comparisons of topographic profiles for parts of Tharsis within the vicinity of Ascraeus Mons at the given latitudes. Dashed lines represent the topography given on the U.S. Geological Survey 1:25 m map of Mars; solid lines show the new radar-derived height estimates presented here. Both data sets are referenced to the 6.1-mbar Mars datum. Radar data are displayed as average elevations for 2° longitude sample bins; most samples contain 5–12 data points, and all mean values have a variance of less than 0.5 km. Breaks in radar profiles are due to absence of returns from those longitudes, presumably due to excessive scattering of the signal by rugged terrain. (*d*) Topographic profiles for Elysium Mons. Data are presented in same format as that used for the Ascraeus Mons data.

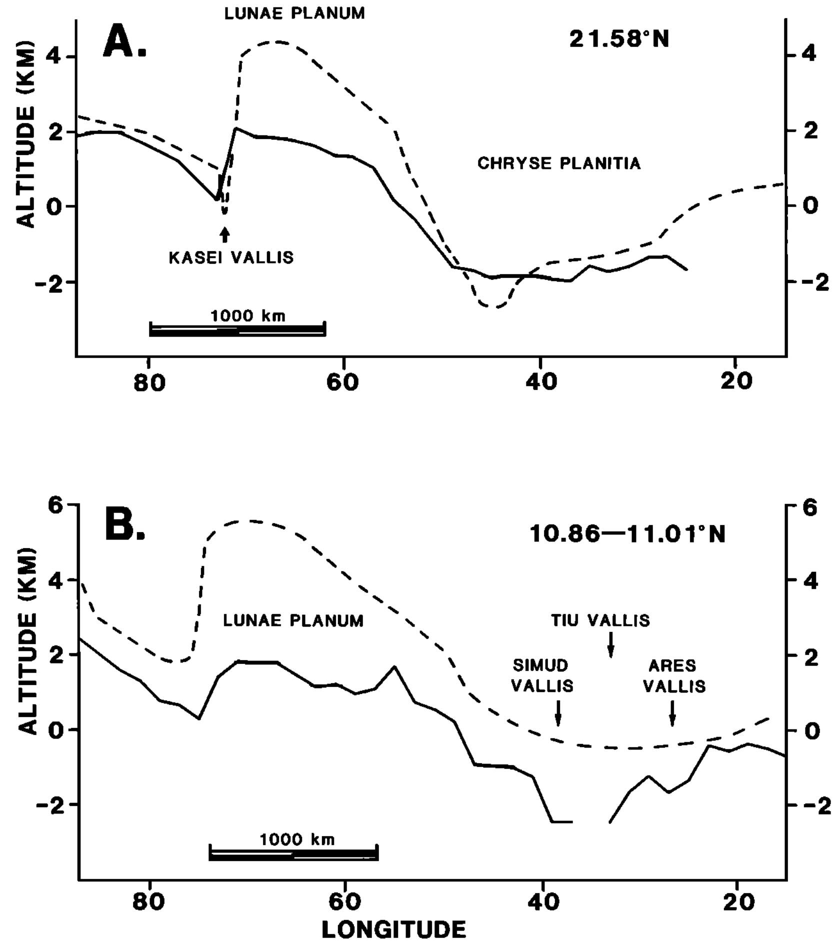

Fig. 3. Comparisons of topographic profiles across Lunae Planum and Chryse Planitia at latitudes of (*a*) 21.58°N and (*b*) 10.86°–11.01°N. The locations of the prominent channel systems are also shown. Data are presented in the same format as that used for Figure 2.

addition to the local geology at Lander 1, the radar data also provide additional topographic information on the channel systems which feed into southern Chryse Planitia, and this will be discussed in more detail below.

Syrtis Major Planitia and Isidis Planitia. Recent interpretations of radar data from the Arecibo Observatory [*Simpson et al.*, 1982] have shown that at 10°N the Syrtis Major/Isidis area is characterized by an abrupt elevation transition from the floor of Isidis (at an elevation of about 2 km below datum) to the ridged plains materials of Syrtis Major (3–4 km above Mars datum). Our data (Figure 4) corroborate this observation and provide additional information on the regional topography to the north and south. As far south as 3°N, Isidis Planitia is depressed below the 6.1-mbar datum, while the plains north of the basin are also 1–1.5 km below the datum. As was noted by *Schaber et al.* [1981], it is also evident that the ridged plains of Syrtis Major are elevated by 0.5–1 km with respect to the cratered terrains to the west. Like Lunae Planum (Figure 3), it therefore seems possible that the lava flows within Syrtis Major were emplaced on top of (and did not replace) the original heavily cratered material and that significant isostatic readjustment has not taken place in either area after these events.

INDIVIDUAL POINTS OF GEOLOGICAL INTEREST

In addition to the profiles presented in Figures 2–4, the new radar elevation data have direct relevance to investigations of a number of diverse geological regions. Topographic data for several such regions are summarized in Table 1. The data have been assigned individual 'entry' numbers to aid in their discussion and are presented as the maximum and mean elevations in the designated 2° longitude bin (the original latitude resolution is retained). The number N of individual measurements and the associated standard deviation (sigma) are listed, except where N equals one.

To provide a more detailed picture of Tharsis, elevation values are given in Table 1 (entries 1–10) for the plains regions surrounding all the major volcanoes. No radar echoes were received from many of the lava flows within Tharsis, apparently because of the very rough surfaces on these flows; most of the incident radar power was evidently very diffusely scattered. Elevation estimates for this region are therefore few in number and probably spatially selected, but they do confirm the lower absolute relief of Tharsis which was described in the previous section. It is also apparent (entries 1, 2, 9, and 10 in Table 1) that in addition to northern Tharsis being generally quite low, the lava plains surrounding Olympus Mons and its aureole are topographically depressed with respect to the surrounding areas. Elevations between −0.1 and +1.3 km are found within 200 km of the southern (entries 9, 10) and northwestern (entry 2) sides of the volcano's basal escarpment; while the eastern base (entry 1) is higher, it is nevertheless only 2 km above the datum. Farther to the south and east, elevations are some-

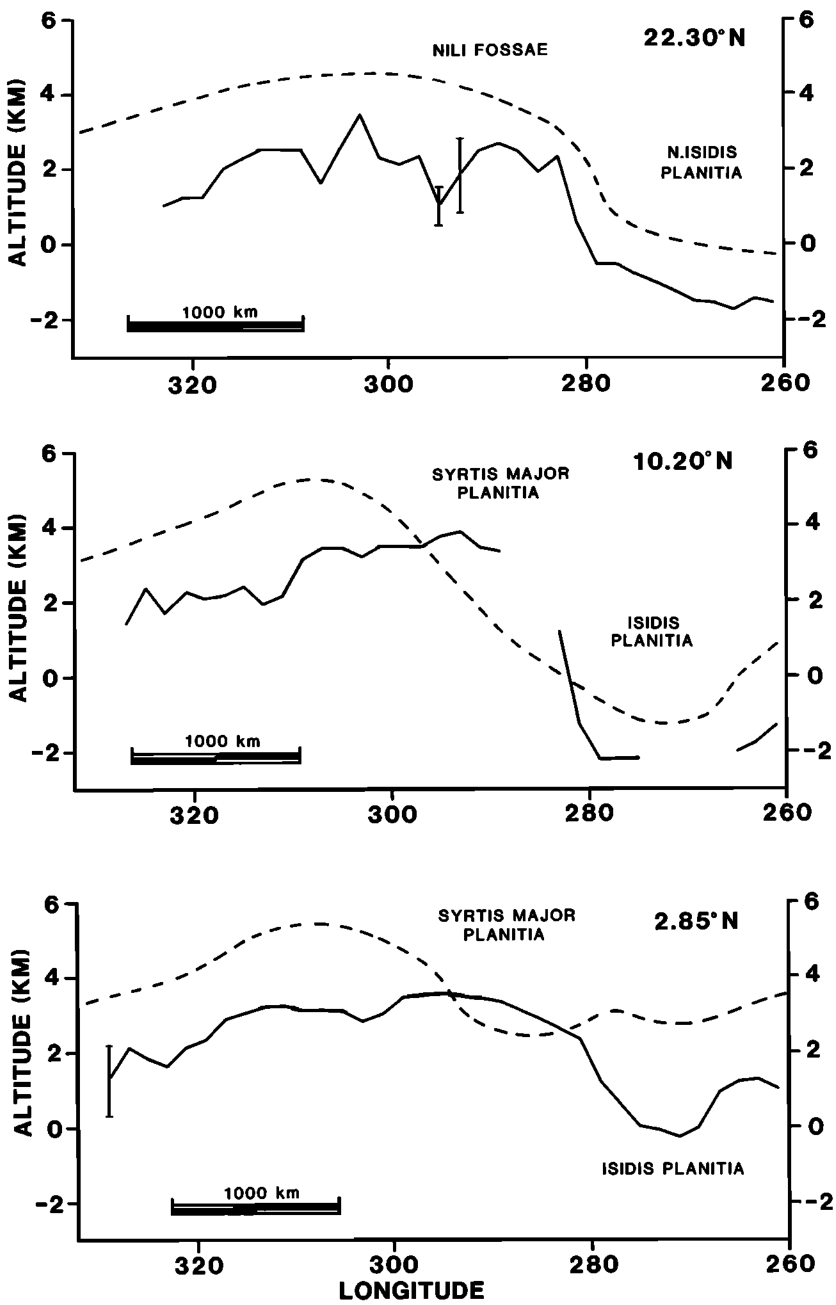

Fig. 4. Comparisons of topographic profiles across Syrtis Major Planitia and Isidis Planitia. Data are presented in the same format as that used for Figure 2, except that error bars (one-sigma values) are also included for data samples with a variance greater than 0.5 km.

what higher, being ~4.3 km and ~2.8 km at an additional 200–250 km in radial directions from the volcano, respectively. The existence of a paleoperipheral depression around Olympus Mons is also suggested by the orientations of lava flows within northwestern Tharsis [*Mouginis-Mark et al.*, 1982], and it may be that such a feature has been preserved since the time when the Tharsis volcanoes were constructed. This depression could be the result of loading by Olympus Mons [*Thurber and Toksöz*, 1978], which has resulted in significant deformation of the surrounding region. Alternatively, the depression may simply have been produced by the combination of the regional slope (down toward the northwest) and the failure of the low-volume lava flows erupted from Olympus Mons [*Mouginis-Mark et al.*, 1982] to extend to distances in excess of 250 km from the basal escarpment.

Radar measurements of the elevations found within Elysium (entries 11–13) and Amazonis planitiae (entries 14, 15) reveal that these parts of the northern plains, together with Chryse Planitia (entries 16, 17), are at a common altitude of about -2 km. All three of these areas are large-scale lava plains which are separated by 5000–10,000 km on the planet, yet evidently share a nearly common elevation. It is unlikely that this attribute is coincidental. A more plausible explanation is the large-scale (low-harmonic) isostatic readjustment of the northern plains after their emplacement. An alternative (and probably more likely) explanation is that areally extensive lavas could have been emplaced upon an older, isostatically compensated surface.

Numerous data points for Chryse Planitia and the large channels to the south (Simud, Ares, and Tiu valles) are included in Table 1 (entries 16–26) to permit an estimate of

TABLE 1. Elevation Estimates for Individual Points of Geological Interest

Entry	Location	Latitude	Longitude	Maximum, km	Mean, km	Sigma, km	N
1	Olympus Mons Aureole	23.14°N	126°–128°W	1.90	1.90	—	1
2	Olympus Mons Aureole	23.14°N	138°–140°W	−0.05	−0.10	0.05?	2
3	S. Tharsis Tholus	10.85°N	88°–90°W	3.25	2.86	0.52	7
4	S. Ascraeus Mons	0.29°N	100°–102°W	7.06	7.06	—	1
5	W. Ceranius Tholus	23.15°N	98°–100°W	4.30	4.29	0.01?	2
6	N. Jovis Tholus	21.43°N	116°–118°W	3.98	3.71	0.19	13
7	Ceranius Fossae	23.15°N	108°–110°W	5.42	5.29	0.07	12
8	N.E. Arsia Mons	6.10°S	114°–116°W	10.18	9.55	0.42	4
9	S. Olympus Mons	12.10°N	136°–138°W	0.75	0.43	0.19	11
10	S. Olympus Mons	11.37°N	136°–138°W	0.99	0.59	0.36	7
11	Hephaestus Fossae	22.13°N	230°–232°W	−2.07	−2.16	0.06	12
12	Elysium Planitia	20.97°N	254°–256°W	−1.86	−2.06	0.15	12
13	Isidis Planitia	10.20°N	276°–278°W	−2.09	−2.20	0.08	11
14	E. Amazonis Planitia	11.37°N	150°–152°W	−1.77	−2.16	0.23	4
15	Amazonis Planitia	9.41°N	160°–162°W	−2.45	−2.52	0.05	11
16	E. Chryse Planitia	21.29°N	36°–38°W	−1.67	−2.04	0.23	10
17	E. Chryse Planitia	21.59°N	44°–46°W	−1.68	−1.88	0.12	13
18	Viking Lander 1	22.71°N	46°–48°W	−1.56	−1.77	0.16	4
19	W. Chryse Planitia	22.71°N	48°–50°W	−0.96	−1.23	0.11	12
20	W. Chryse Planitia	22.71°N	50°–52°W	−0.66	−0.91	0.15	5
21	W. Chryse Planitia	21.59°N	46°–48°W	−1.48	−1.69	0.12	12
22	W. Chryse Planitia	21.59°N	48°–50°W	−1.05	−1.58	0.28	13
23	W. Chryse Planitia	21.59°N	50°–52°W	−0.68	−0.94	0.13	12
24	Simud Vallis	10.19°N	36°–38°W	−2.17	−2.46	0.19	11
25	Ares Vallis	9.98°N	24°–26°W	−0.99	−1.25	0.19	7
26	Tiu Vallis	10.20°N	32°–34°W	−1.18	−2.29	0.44	11
27	N. Noctis Labyrinthus	6.10°S	98°–100°W	9.17	9.04	0.11?	3
28	Tithonia Catena	6.10°S	82°–84°W	6.02	5.97	0.06?	2
29	W. Echus Chasma	0.28°N	84°–86°W	4.17	3.95	0.18	4
30	E. Eos Chasma	15.00°S	36°–38°W	2.18	1.94	0.15	12

Each data point has been given an 'entry' number to aid its discussion in the text. Data are maximum and average values for 2° longitude sample bins. One–standard deviation (sigma) values for the mean and the number of data points (*N*) within each sample are also given. All elevations are referenced to the 6.1-mbar Mars datum.

the modern-day channel slopes. Of particular interest is the fact that the radar data show that the preserved sections of Simud and Tiu valles are actually lower (by 600–800 m) than many parts of their outwash plains within southern Chryse Planitia. Assuming that no deformation of the floor of Chryse Planitia has occurred since the time of channel formation, the greater depths of the valleys compared to those of the deltas suggest that the channel floors may have been overdeepened during their formation, possibly due to the creation of the valleys by ice streams rather than liquid water [*Lucchitta et al.*, 1981].

The radar data show that the relief of Valles Marineris is extreme. Previous radar measurements [*Roth et al.*, 1980] have indicated that the canyon is more than 6 km deep; our data demonstrate that the rim (entries 27–30) also has a pronounced regional tilt (down toward the east). North of Noctis Labyrinthus (6°S, 100°W; entry 27) the surrounding plains are at an elevation of about 9 km, while at the eastern end of Eos Chasma, 3600 km to the east, the rim is only about 2 km above the datum (entry 30). A pair of height measurements on the northern rim of the canyon at Tithonia Catena (entry 28) was also obtained during the radar measurements, thereby providing an independent control point for the recently published 1:500,000 topographic map of Tithonium Chasma (U.S. Geological Survey miscellaneous map I-1294).

Discussion of Data Set Discrepancies

Because the elevation values reported here differ significantly from those given on the U.S. Geological Survey topographic map of Mars, it is pertinent to consider additional independently derived estimates of elevation and the possible cause of the reported discrepancies. Viking radio occultation measurements [*Lindal et al.*, 1979] provide one such independent data set, with a few point estimates of elevation (with an estimated accuracy of 1 km) almost coincident with the radar groundtracks. A comparison of these coincident radar and occultation measurements (Table 2) demonstrates that in most instances the maximum radar-derived height estimate is within 500 m of the occultation value. Because occultation measurements are always biased toward the highest local surface elevation (due to the spacecraft's signal being lost behind the highest feature along the line of sight [*Lindal et al.*, 1979]), the discrepancies shown in Table 2 are not considered to be significant. Overestimates of the occultation-derived elevations were predicted to be greatest for areas of rough terrain or in the proximity of major topographic features, such as the huge volcanoes. In these instances it is likely that the maximum elevation estimate from the radar (rather than the mean value) is the closest comparison to the occultation measurements listed in Table 2.

As was mentioned above, the U.S. Geological Survey map also employed radio occultation data (in this case, data from Mariner 9 [*Kliore et al.*, 1973]) as the major part of the control information for the northern hemisphere [*Wu*, 1978]. However, both this map and the topographic map produced by *Christensen* [1975] (which utilized essentially similar data sets but differed in the estimated bias assigned to each data set) overestimated the elevations of Tharsis, Lunae Planum,

TABLE 2. Comparison of Elevation Determinations From Viking Orbiter Radio Occultations and the Present Radar Data Set

Location			Radar Elevation			
Latitude	Longitude	Occultation*	Maximum, km	Mean, km	Sigma	N
22.52°N	34°–36°W	−0.1	−1.20	−1.37	0.18	4
21.81°N	252°–254°W	−1.9	−1.72	−1.83	0.09	12
11.29°N	32°–34°W	−0.1	0.04	−1.61	0.76	11
10.29°N	336°–338°W	2.3	2.26	2.10	0.10	5
2.22°N	174°–176°W	1.2	1.31	−0.05	1.36?	2
5.90°S	342°–344°W	3.2	2.67	2.48	0.15	4
17.66°S	180°–182°W	3.0	3.53	2.98	0.31	13
18.09°S	56°–58°W	4.0	3.46	3.34	0.08	13
21.97°S	314°–316°W	4.5	4.21	3.90	0.17	10

Each height estimate has been given an 'entry' number to aid its discussion in the text. Occultation values are single-point estimates with an estimated accuracy of about 1 km; radar data are presented in the same format as that used for Table 1.

*Occultation estimates of surface elevation from *Lindal et al.* [1979].

Elysium, and Syrtis Major by amounts varying from 2 to 5 km compared to the radar data. It is therefore interesting to consider the possible reasons for this discrepancy in the elevation estimates.

An examination of the distribution of the Mariner 9 occultation measurements [*Kliore et al.*, 1973, their Figure 1] reveals that no occultation data were obtained for any of the above-mentioned localities where elevation discrepancies of several kilometers exist. We therefore infer that the Mariner 9 infrared interferometer spectrometer (IRIS) and ultraviolet spectrometer (UVS) experiments provided the elevation control information in these regions. Comparing the different data sets, the differences in elevation appear to be greatest over high-altitude regions and areas of ridged plains materials [*Scott and Carr*, 1978]. This suggests that the observed infrared characteristics of the surface [*Hanel et al.*, 1972], or the UVS scattering [*Hord et al.*, 1972, 1974], were different from those predicted by the theoretical models. One possible cause for such a difference is that the Martian surface may have a systematically lower emissivity (or UV reflectivity) at higher elevations because of the differences either in material properties or in the amount of condensate masking of the surface or because of an unexpected elevation-dependent component in the atmosphere.

If the noted effect is one of systematic variations in atmospheric scattering, there is a possibility of interpreting the inferred elevation differences in terms of topographically controlled atmospheric phenomena. Low-altitude winds could entrain more dust than can be supported at high altitudes. Alternatively, if the observed variations in elevation can be shown to be a consequence of differences in surface UV reflectivity, then it would require an elevation dependence of surface geochemistry to explain the discrepancy, which could be confirmed from the multispectral reflectivity properties of various mineral types. While in the present study our attention has focused on the geomorphology of the surface, it appears that the new radar data set also presents intriguing possibilities for investigating other Martian phenomena.

CONCLUSIONS AND IMPLICATIONS

The new radar measurements of elevations within the northern hemisphere of Mars have direct relevance to numerous geophysical and morphological investigations currently of general interest. It appears, for example, that a reanalysis of the geophysical and petrological evolution of the Tharsis region should be conducted to include the lower measured elevations of the 'Tharsis dome.' Models which are based either on the constructional growth or on the regional uplift of Tharsis will have to account for the much lower elevation (2–4 km above datum) of the lava plains surrounding Ascreaus Mons. The question of construction versus uplift does not totally disappear with the data described here, however, because plains materials within Syria Planum and north of Noctis Labyrinthus attain altitudes of about 9 km. Thus in areas where no volcanic constructs can be recognized, the surface of Mars is over 5 km higher than within the central portion of Tharsis where the young volcanoes are found.

Accompanying such a reanalysis of Tharsis topography, it also appears that the Bouguer-corrected gravity models for this area may need further investigation. Since the lower elevations will make the correction smaller, the uncompensated mass concentration is even larger than has previously been thought, making the support mechanism for this area even more enigmatic. Similar considerations apply to Elysium and Isidis planitae, as well as Lunae Planum, although the extremely large mass concentrations are not present.

A variety of previous correlations between topography and morphological features are also affected. For example, the apparent correlation of impact crater ejecta morphologies with elevation [*Mouginis-Mark*, 1979] will undoubtedly need modification. On the other hand, the new radar data also provide the potential for several new, more rigorous investigations of the Martian surface than were previously possible. The derivation of local slopes for the large channels feeding Chryse Planitia can now be conducted, while searches for erosion surfaces and ancient impact basins within the cratered hemisphere are also feasible.

Acknowledgments. The indispensible assistance of C. Franck, G. Morris, and the Radio Science Support Group (Goldstone) in acquiring the data presented here is gratefully acknowledged. Comments by R. Simpson and J. Head helped improve an earlier version of the manuscript. This paper presents the results of one phase of the research carried out at the Jet Propulsion Laboratory, California Institute of Technology, under contract NAS 7-100, sponsored by the U.S. National Aeronautics and Space Administration.

REFERENCES

Carr, M. H., Tectonism and volcanism of the Tharsis region of Mars, *J. Geophys. Res.*, *79*, 3943–3949, 1974.

Christensen, E. J., Martian topography derived from occultation, radar, spectral, and optical measurements, *J. Geophys. Res.*, *80*, 2909–2913, 1975.

De Hon, R. A., Thickness of volcanic materials on the eastern flank of the Tharsis Plateau (abstract), in *Papers presented to the Third International Colloquium on Mars*, pp. 59–61, Lunar and Planetary Institute, Houston, Tex., 1981.

Downs, G. S., P. E. Reichley, and R. R. Green, Radar measurements of Martian topography and surface properties: The 1971 and 1973 oppositions, *Icarus*, *26*, 273–312, 1975.

Garvin, J. B., P. J. Mouginis-Mark, and J. W. Head, Characterization of rock populations on planetary surfaces: Techniques and a preliminary analysis of Mars and Venus, *Moon Planets*, *24*, 355–387, 1981.

Hanel, R., B. Conrath, W. Hovis, V. Kunde, P. Lowman, W. Maguire, J. Pearl, J. Pirraglia, C. Prabhakara, B. Schlachman, G. Levin, P. Straat, and T. Burke, Investigation of the martian environment by infrared spectroscopy on Mariner 9, *Icarus*, *17*, 423–442, 1972.

Hord, C. W., C. A. Barth, A. I. Stewart, and A. L. Lane, Mariner 9 ultraviolet spectrometer experiment: Photometry and topography of Mars, *Icarus, 17,* 443–456, 1972.

Hord, C. W., K. E. Simmons, and L. K. McLaughlin, Mariner 9 ultraviolet spectrometer experiment: Pressure-altitude measurements on Mars, *Icarus, 21,* 292–302, 1974.

Kliore, A. J., D. L. Cain, G. Fjeldbo, and B. L. Seidel, Mariner 9 *S*-band Martian occultation experiments: Initial results on the atmosphere and topography of Mars, *Science, 175,* 313–317, 1972.

Kliore, A. J., G. Fjeldbo, B. L. Seidel, M. J. Sykes, and P. M. Woiceshyn, *S*-band radio occultation measurements of the atmosphere and topography of Mars with Mariner 9: Extended mission coverage of the polar and intermediate latitudes, *J. Geophys. Res., 78,* 4331–4351, 1973.

Lambeck, K., Comments on the gravity and topography of Mars, *J. Geophys. Res., 84,* 6241–6247, 1979.

Lindal, G. F., H. B. Hotz, D. N. Sweetnam, Z. Shippony, J. P. Brenkle, G. V. Hartsell, R. T. Spear, and W. H. Michael, Viking radio occultation measurements of the atmosphere and topography of Mars: Data acquired during 1 Martian year of tracking, *J. Geophys. Res., 84,* 8443–8456, 1979.

Lucchitta, B. K., D. W. Anderson, and H. Shoji, Did ice streams carve martian outflow channels?, *Nature, 290,* 759–763, 1981.

Mouginis-Mark, P. J., Martian fluidized crater morphology: Variations with crater size, latitude, altitude, and target material, *J. Geophys. Res., 84,* 8011–8022, 1979.

Mouginis-Mark, P. J., and S. H. Brown, An unusual volcanic center in western Elysium Planitia, Mars (abstract), *Lunar Planet. Sci., 12,* 729–731, 1981.

Mouginis-Mark, P. J., S. H. Zisk, and G. S. Downs, Ancient and modern slopes in the Tharsis region of Mars, *Nature, 297,* 546–550, 1982.

Phillips, R. J., and K. Lambeck, Gravity fields of the terrestrial planets: Long-wavelength anomalies and tectonics, *Rev. Geophys. Space Phys., 18,* 27–76, 1980.

Phillips, R. J., and R. S. Saunders, The isostatic state of Martian topography, *J. Geophys. Res., 80,* 2893–2897, 1975.

Phillips, R. J., R. S. Saunders, and J. E. Conel, Mars: Crustal structure inferred from Bouguer gravity anomalies, *J. Geophys. Res., 78,* 4815–4820, 1973.

Pike, R. J., and G. D. Clow, Martian volcanoes in a classification of central edifices (abstract), in *Paper presented to the Third International Colloquium on Mars,* pp. 199–201, Lunar and Planetary Institute, Houston, Tex., 1981.

Roth, L. E., G. S. Downs, R. S. Saunders, and G. Schubert, Radar altimetry of South Tharsis, Mars, *Icarus, 42,* 287–316, 1980.

Schaber, G. G., K. L. Tanaka, and J. K. Harmon, Syrtis Major revisited: A highland volcanic planum, not a planitia (abstract), in *Papers presented to the Third International Colloquium on Mars,* pp. 223–225, Lunar and Planetary Institute, Houston, Tex., 1981.

Scott, D. H., and M. H. Carr, Geologic map of Mars, *Misc. Map I-1083,* U.S. Geol. Surv., Reston, Va., 1978.

Simpson, R. A., G. L. Tyler, J. K. Harmon, and A. R. Peterfreund, Radar measurements of small-scale surface texture: Syrtis Major, *Icarus, 49,* 258–283, 1982.

Sleep, N. H., and R. J. Phillips, An isostatic model of the Tharsis province, Mars, *Geophys. Res. Lett., 6,* 803–806, 1979.

Solomon, S. C., and J. W. Head, Tharsis province: Uplift by anomalous mantle, or concentration of tectonism and volcanism in a locally thin lithosphere? (abstract), *Lunar Planet. Sci., 11,* 1063–1065, 1980.

Thurber, C. H., and M. N. Toksöz, Martian lithospheric thickness from elastic flexure theory, *Geophys. Res. Lett., 5,* 977–980, 1978.

Wise, D. U., M. P. Golombek, and G. E. McGill, Tharsis province of Mars: Geologic sequence, geometry, and a deformation mechanism, *Icarus, 38,* 456–472, 1979*a*.

Wise, D. U., M. P. Golombek, and G. E. McGill, Tectonic evolution of Mars, *J. Geophys. Res., 84,* 7934–7939, 1979*b*.

Wu, S. S. C., Mars synthetic topographic mapping, *Icarus, 33,* 417–440, 1978.

(Received December 4, 1981;
accepted April 23, 1982.)